FATIGUE BEHAVIOR OF Al-Mg-Mn ALLOY WITH MINOR ADDITIONS OF SCANDIUM AND ZIRCONIUM

A project report submitted in partial fulfillment of the requirement for the award of the degree of

BACHELOR OF TECHNOLOGY

In

MECHANICAL ENGINEERING

By

BODDEPALLI CHANDRASEKHAR SAI SRINIVAS	**318126520120**
BOKAM CHANDRA MOULI	**318126520121**
SOPETI MADHU SUDHANA RAO	**318126520165**
CHALUMURU SAI PRASAD	**318126520127**
DWARA SRIMANTH	**318126520136**

Under the guidance of

Dr. SRINIVASA RAO MALLIPUDI, Ph. D., MIE., MISTE.

Assistant Professor

Department of Mechanical Engineering

ANIL NEERUKONDA INSTITUTE OF TECHNOLOGY & SCIENCES
(Permanently affiliated to Andhra University, approved by AICTE, Accredited by NBA & NAAC) Sangivalasa – 531162, Bheemunipatnam (Mandal), Visakhapatnam (District), Andhra Pradesh, India.

2022

ANIL NEERUKONDA INSTITUTE OF TECHNOLOGY& SCIENCES (A)

Sangivalasa, Bheemunipatnam (Mandal), Visakhapatnam-531162.

PRAGNANAM BRAHMA

ANITS

CERTIFICATE

This is to certify that the project report entitled "**Identification of Optimal Processing Parameters in CNC Turning of AA6061 Using Taguchi technique**" has been carried out by **Golla Nikhil Durga Sai (318126520138), Tutika Ganesh (319126520L23), Chikka Sai Surya (318126520129), Doddi Revanth (318126520135), Botcha Bharadwaj Srinivas (318126520125)** under the esteemed guidance of **Dr. M.PRASANTH KUMAR**, in partial fulfilment of the requirements for the award of the Degree of Bachelor of Technology in Mechanical Engineering by Anil Neerukonda Institute Of Technology & Sciences(A), Visakhapatnam.

PROJECT GUIDE

23/5/22

(Dr.M.Prasanth Kumar)

Assistant Professor

Dept. of Mechanical Engineering

ANITS, Sangivalasa

Visakahapatnam.

APPROVED BY:

28.5.22

(Prof. & Dr.B.Naga Raju)

Head of the Department

Dept. Of Mechanical Engineering

ANITS, Sangivalasa

Visakhapatnam.

PROFESSOR & HEAD
Department of Mechanical Engineering
ANIL NEERUKONDA INSTITUTE OF TECHNOLOGY & SCIENCES
Sangivalasa 531 162 VISAKHAPATNAM Dist. A.P.

THIS PROJECT IS APPROVED BY THE BOARD OF EXAMINERS

INTERNAL EXAMINER:

PROFESSOR & HEAD
Department of Mechanical Engineering

EXTERNAL EXAMINER:

ACKNOWLEDGEMENT

I express immensely my deep sense of gratitude to **Dr. SRINIVASA RAO MALLIPUDI**, Assistant professor, Department of Mechanical Engineering, Anil Neerukonda institute of Technology and Sciences, Sangivalasa, Visakhapatnam district for his valuable guidance and encouragement at every stage of the work made it a successful fulfilment.

Also, we are very thankful to **Prof. T. V. Hanumantha Rao** Principal, **Dr. B. Naga Raju**, Head of the Department, Mechanical Engineering, Anil Neerukonda Institute of Technology and Sciences, Visakhapatnam.

We express sincere thanks to the members of Teaching and Non- Teaching staff of the Department of Mechanical Engineering, ANITS, for their co-operation and support to carry on work.

We acknowledge the people who mean a lot to me, my parents, for showing faith in me and giving me liberty to choose what we desired. We salute you all for the selfless love, care, pain and sacrifice you did to shape my life.

BODDEPALLI CHANDRA SEKHAR (318126520120)

BOKAM CHANDRA MOULI (318126520121)

SOPETI MADHU SUDHANA RAO (318126520165)

CHALUMURU SATYA SAI PRASAD (318126520127)

DWARA SRIMANTH (318126520136)

ABSTRACT

The present project deals with study of fatigue life of Al-Mg-Mn alloy with and without minor additions of Sc and Zr. The investigated Aluminum alloy which is cold rolled, tensile testing is done and then fatigue life of the investigated alloy is determined. Failure of the specimen at different stresses applied is determined and the number of cycles to failure is noted. Fatigue has become progressively more prevalent as technology has developed a greater amount of equipment subject to repeated loading and vibration. In our experiment the Al-Mg-Mn alloy with minor additions of Sc and Zr were produced by stir casting to form plates and treated with cold rolling. The tensile testing of the specimen was done in INSTRON 8801. The results obtained from this test says that yield strength of the Al-Mg-Mn-Sc-Zr alloy was found to be more than the Al-Mg-Mn alloy. The failure of the specimen here occurs at a very large number of cycles. On the order of 10^4, this number of cycles decreases with an increase in the applied stress. As the load increases the failure of the specimen would occur at a smaller number of cycles. This alloy used fails at a large number of cycles. So, for use of this alloy a large number of cycles is required and also a lower yield stress. This aluminum alloy can be used for a large number of uses. Aircraft application, gas pipelines, oil tanks, pistons, etc.

Keywords:- Fatigue, alloy, Aluminum, cyclic load. Al-Mg-Mn-Sc-Zr, Al-Mg-Mn

CONTENTS

LIST OF FIGURES

LIST OF TABLES

1 INTRODUCTION

1.1 INTRODUCTION OF ALUMINUM ALLOYS

The development of lightweight metals in the field of engineering and technology is due to the demand for such high strength to weight ratio materials in aerospace, automotive and marine applications. Wrought Aluminum alloys were come under this category to fulfill the requirement for such applications.

1.2 CLASSIFICATION OF WROUGHT ALUMINIUMALLOYS

Wrought Aluminum alloys are generally classified as strain-hardening alloys and age-hardening alloys and the detailed classification is shown in Figure1.1. In Wrought Aluminum alloy designation system, the first digit refers to the main alloying elements, the second digit gives the modification in that alloy, the third and fourth digits give the individual alloy variations and identification of the alloy in that group. The strain-hardening alloys (1xxx, 3xxx, 4xxx and 5xxx alloy series are non-heat treatable). The strength of these alloys may be improved by strain hardening technique. The age-hardening alloys (2xxx, 6xxx and 7xxx alloy series). These alloys improved their properties by heat treatment and quenching followed by natural or artificial aging.

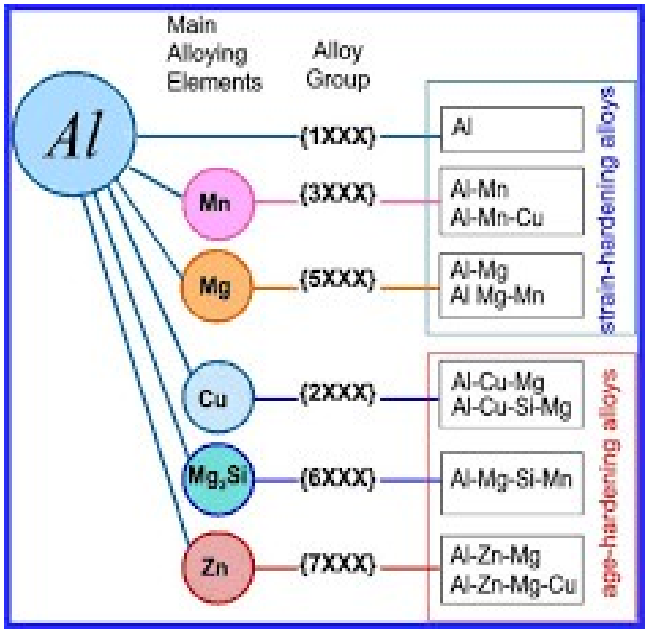

Fig 1.1 Classification of Aluminum Alloys

1.3 ALUMINIUM ALLOY CHOSEN FOR THEPRESENT STUDY

In this project work, a 5xxx series alloy is chosen for the investigation. This alloy usually contains aluminum (Al), magnesium (Mg), manganese (Mn) as principal alloying constituents and traces of other metals. This alloy attains medium strength and high corrosion resistance among all the non-heat treatable alloys, derives their strength primarily from solid solution strengthening by Mg and Mn. Increase in the Mg content in this series of alloys leads to increase in tensile strength, Mn increases corrosion resistance due to the presence of Al_3Mg_2, Mg_2Si, $Al_6(Fe, Mn)$ intermetallics. These alloys are work-hardenable and can be easily drawn into any shape due to high formability, and exhibits high ductility, good weldability, durability, and good finishing characteristics. Thus, these alloys were used in many chemical industries, ship buildings, naval and marine applications. Medium strength is the limitation for these alloys. Al-Mg-Mn alloys are often strengthened by work hardening/strain hardening strengthening, solid solution strengthening, grain refinement strengthening and precipitate strengthening mechanisms. Amongst different strengthening mechanisms for Al-Mg-Mn alloys, Minor-alloying strengthening is an alternative way, which involves the addition of alloying elements such as Ti, Fe, Er, Cr, Mn, Cu, Zn, Ni, Hf, Zr, and Sc as an alloying element. In the present study, Al-Mg-Mn alloy containing the traces of Sc and Zirconium is considered.

1.4 INTRODUCTION TO FATIGUE

It has been recognized since 1830 that a metal subjected to a repetitive or fluctuating stress will fail at a stress much lower than that required to cause fracture on a single application of load. Failures occurring under conditions of dynamic loading are called fatigue failures, presumably because it is generally observed that these failures occur only after a considerable period of service. Fatigue has become progressively more prevalent as technology has developed a greater amount of equipment, such as automobiles, aircraft, compressors, pumps, turbines, etc., subject to repeated loading and vibration. Today it is often stated that fatigue accounts for at least 90 percent of all service failures due to mechanical causes.

1.5 STRUCTURAL FEATURES OF FATIGUE FAILURE

A fatigue failure is particularly insidious because it occurs without any obvious warning. Fatigue results in a brittle-appearing fracture, with no gross deformation at the fracture. On

macroscopic scale the fracture surface is usually normal to the direction of the principal tensile stress. A fatigue failure can usually be recognized from the appearance of the fracture surface, which shows a smooth region, due to the rubbing action as the crack propagated through the section, and a rough region, where the member has failed in a ductile manner when the cross section was no longer able to carry the load. Frequently the progress of the fracture is indicated by a series of rings, or "beach marks", progressing inward from the point of initiation of the failure.

One can determine that a material failed by fatigue by examining the fracture sight. A fatigue fracture will have two distinct regions; One being smooth or burnished as a result of the rubbing of the bottom and top of the crack. These visual clues may be seen in figure 1.2.

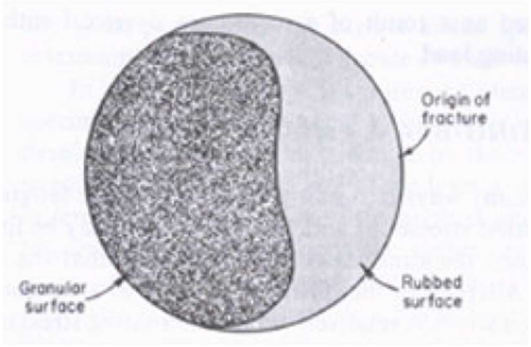

Fig 1.2 Fatigue Visual Clues

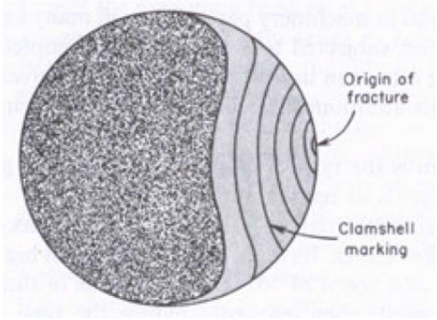

Fig 1.3 Beachmarks and Striations

Notice that the rough surface indicates brittle failure, while the smooth surface represents crack propagation Other features of a fatigue fracture are beach marks and striations. Beachmarks, or clamshell marks, may be seen in fatigue failures of materials that are used for a period of time, allowed to rest for an equivalent time period and then loaded again as in factory usage. Striations are thought to be steps in crack propagation, where the distance depends on the stress range. Beachmarks may

contain thousands of striations. Visual Examples of Beachmarks and Striations are seen below in Figure. 1.2 and 1.3

1.6 FACTORS CAUSING FATIGUE FAILURE

Three basic factors are necessary to cause fatigue failure. These are:

- Maximum tensile stress of sufficiently high value,
- Large enough variation or fluctuation in the applied stress, and
- Sufficiently large number of cycles of the applied stress.

In addition, there are a host of other variables, such as stress concentration, corrosion, temperature, overload, metallurgical structure, residual stresses, and combined stresses, which tend to alter the conditions for fatigue. Since we have not yet gained a complete understanding of what causes fatigue in metals, it will be necessary to discuss each of these factors from an essentially empirical standpoint.

1.7 STRESS CYCLES

At the outset it will be advantageous to define briefly the general types of fluctuating stresses which can cause fatigue. Figure 1.4(a) serves to illustrate typical fatigue stress cycles. Figure 1.4(b) illustrates a completely reversed cycle of stress of sinusoidal form. For this type of stress cycle the maximum and minimum stresses are equal. Tensile stress is considered positive, and compressive stress is negative. Figure 4b illustrates a repeated stress cycle in which the maximum stress σmax (Rmax) and minimum stress σmin (Rmin) are not equal. In this illustration they are both tensions, but a repeated stress cycle could just as well contain maximum and minimum stresses of opposite signs or both in compression. Figure 1.4(c) illustrates a complicated stress cycle which might be encountered in a part such as an aircraft wing which is subjected to periodic unpredictable overloads due to gusts.

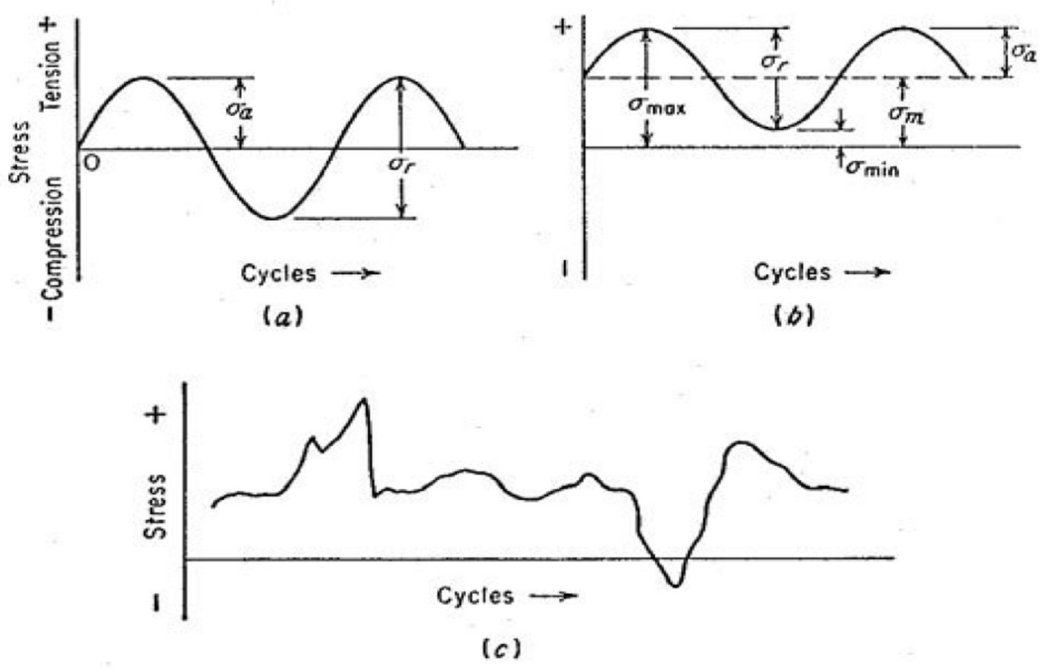

Fig 1.4 Typical fatigue stress cycles; (a) Reversed stress; (b) repeated stress; (c)

1.8 S-N CURVE

The basic method of presenting engineering fatigue data is by means of the S-N curve, a plot of stress S against the number of cycles to failure N. A log scale is almost always used for N. The value of stress that is plotted can be _a, _max, or _min. The stress values are usually nominal stresses, The highest stress at which a run out (non-failure) is obtained is taken as the fatigue limit.

For materials without a fatigue limit the test is usually terminated for practical considerations at a low stress where the life is about 10^8 or $5x10^8$ cycles. The S-N curve is usually determined with about 8 to 12 specimens.

1.9 LOW-CYCLE FATIGUE

The engineering failures which occur at relatively high stress and low numbers of cycles to failure. This type of fatigue failure is called low cycle fatigue failure and must be considered in the design of nuclear pressure vessels, steam turbines, and most other types of power machinery. Low-cycle fatigue conditions frequently are created where the repeated stresses are of thermal origin. Since thermal

stresses arise from the thermal expansion of the material, it is easy to see that in this case fatigue results from cyclic strain rather than from cyclic stress.

1.10 HIGH CYCLE FATIGUE

High Cycle Fatigue (HCF) results from vibratory stress cycles at frequencies which can reach thousands of cycles per second and can be induced from various mechanical sources. It is typical in aircraft gas turbine engines and has led to the premature failure of major engine components (fans, compressors, turbines). While LCF involves bulk plasticity where stress levels are usually above the yield strength of the material, HCF is predominantly elastic, and stress levels are below the yield strength of the material.

1.11 FATIGUE OF ALUMINUM ALLOYS

Aluminum alloys or aluminum alloys are alloys of aluminum often with copper, zinc, manganese, silicon, or magnesium. They are much lighter and more corrosion resistant than plain carbon steel but not quite as corrosion resistant as pure aluminum. Bare aluminum alloy surfaces will keep their apparent shine in a dry environment, but light amounts of corrosion products rub off easily onto skin when touched. Galvanic corrosion can be rapid when aluminum alloy is placed in proximity to stainless steel in a wet environment. Aluminum alloy and stainless-steel parts should not be mixed in water containing systems or outdoor installations. When these alloys are subjected to thermal treatment failure on its surface will be there, which would lead to failure of the material. The fatigue crack growth of metallic materials is widely considered to be affected by both intrinsic and extrinsic contributions to propagation resistance Extrinsic resistance to propagation is identifiable with a variety of micromechanical effects which can reduce the crack tip driving force, with crack closure (and associated compressive load transfer in the crack wake being identified as a major influence on crack growth resistance in various material/load condition.

It has been seen that the endurance limit for aluminum metal is not present and thus is taken at a number of cycles of the order 108.due to the presence of interstitial elements in these alloys, no fatigue limit is seen. Performance of these aluminum alloys are taken by noting its crack growth rate ((da/dN) as a function of stress intensity factor K.

This property of aluminum alloys is used in various applications such as aircrafts, space shuttles, marine purpose r cars, trains; offshore structures etc. The alloy standards for aluminum are set by the society of automotive engineer's standards organization, specifically its aerospace standards subgroups.

1.12 APPLICATIONS

1. Aerospace.
2. Automobile.
3. Marine.
4. Ship building.

2 LITERATURE REVIEW

2.1 STUDIES

Norman et al. (2003) investigated that small addition of scandium (Sc) in Al-aerospace alloys (AA2024 and AA7475). They studied the mechanical properties of these alloys.

It has been reported that small additions of scandium (Sc) can improve the weldability and mechanical properties of some aluminum aerospace alloys that are normally considered to be 'unweldable'. In order to determine the mechanisms by which these improvements occur, and more rapidly arrive at optimum Sc addition levels, small wedge-shaped castings have been used to simulate the cooling rates found in MIG/TIG welds. Using this technique, a range of Sc addition levels have been made to two typical Al-aerospace alloys, 2024 and 7475. It has been found that when the Sc level exceeds a critical concentration, small Al3Sc primary particles form in the melt and act as very efficient grain nucleants, resulting in simulated fusion zone grain sizes as fine as 15 μm. This exceptional level of grain refinement produced an unusual grain structure that exhibited no dendritic, or cellular, substructure and a large increase in strength and ductility of the castings. Sc also produced changes in the alloy's freezing paths, which cannot yet be fully explained, but led to the appearance of the W phase in the 2024 alloy and, in both alloys, an overall reduction in the amount of eutectic formed during solidification. When coupled with the high level of grain refinement, this behavior could be used to explain the increased strength and ductility of the castings. In 2000 and 7000 series aluminum alloys, it is therefore anticipated that optimized Sc bearing filler wires will significantly improve the mechanical properties of the weld metal, as well as reducing the tendency for solidification cracking.

Polmear(2006) Al-Mg-Mn alloys are widely used for their good formability. In the annealed state, these alloys exhibit low-to-moderate strengths ranging from 90 to 160 MPa for different Mg contents.

Belov et al.(2007) studied the Al-Mg-Mn alloys with additions of Sc-Zr. They observed that the Al-Mg-Mn-Sc-Zr was a promising light-weight material in the class of Aluminum alloys can be used in low-density systems which exhibit high strength and corrosion resistance.

PENG, Yong-yi (2007) studied that the addition of Sc and Zr decreases activation energy and improves the superplastic property of Al-Mg-Mn alloy. The addition of Sc and Zr refines the grain structure greatly.

The effect of Sc and Zr on the superplastic properties of Al-Mg-Mn alloy sheets was investigated by a control experiment. The superplastic properties and the mechanism of superplastic deformation of the two alloys were studied by means of optical microscope, scanning electron microscope and transmission electron microscope. The elongation to failure of Al-Mg-Mn-Sc-Zr alloy is larger than that of Al-Mg-Mn alloy at the same temperature and initial strain rate. The variation of strain rate sensitivity index is similar to that of elongation to failure. In addition, Al-Mg-Mn-Sc-Zr alloy exhibits higher strain rate superplastic properties. The activation energies of the two alloys that are calculated by constitutive equation and linear regression method approach the energy of grain boundary diffusion. The addition of Sc and Zr decreases activation energy and improves the superplastic property of Al-Mg-Mn alloy. The addition of Sc and Zr refines the grain structure greatly. The main mechanism of superplastic deformation of the two alloys is grain boundary sliding accommodated by grain boundary diffusion. The fine grain structure and high density of grain boundary, benefit grain boundary sliding, and dynamic recrystallization brings new fine grain and high angle grain boundary which benefit grain boundary sliding too. Grain boundary diffusion, dislocation motion and dynamic recrystallization harmonize the grain boundary sliding during deformation.

C Watanabe (2009) Al-Mg-Sc alloy polycrystals bearing Al3Sc particles with different sizes, i.e. 4, 6 and 11 nm in diameter, have been cyclically deformed at 423 K under constant plastic-strain amplitudes, and the microstructural evolution has been investigated in relation to the stress-strain response. Cyclic softening after initial hardening is found in specimens with small particles of 4 and 6 nm, but no cyclic softening takes place in specimens with larger particles of 11 nm. These features of cyclic deformation behavior are similar to the results previously obtained at room temperature. Transmission electron microscopy observations reveal that dislocations are uniformly distributed under all applied strain amplitudes in the specimens containing large particles of 11 nm. The 6 and 11 nm Al3Sc particles have a stronger retardation effect on the formation of fatigue-induced stable dislocation structure than 4 nm particles at 423 K.

Zhang Zhijun (2009) The room temperature high-cycle fatigue performance of Al-4.7Mg-0.7Mn-0.4Er-0.1Zr alloy sheet is studied, and the fatigue performance of the alloy is calculated by the lifting method. The strength is 293.6MPa. Scanning electron microscopy was used to observe the morphological characteristics of the fracture surface of the fatigue specimen, and the cause of fatigue cracks and the process of fatigue fracture were analyzed.The results show that after the addition of erbium and zirconium, nano-sized spherical Al3Er particles are formed inside the alloy, and the fatigue strength of the alloy at room temperature is significantly improved.

Huizhong Li (2010) The effects of micro-alloying with small amounts of Sc and Nd elements on the microstructure and mechanical properties of Al-Mg-Mn alloy were systematically investigated. The results show that the grains of Al-Mg-Mn alloy can be refined by the addition of minor Sc and Nd. Adding 0.2 wt.% Sc or 0.2 wt.% Nd element to Al-Mg-Mn alloy can improve the strength

The effects of micro-alloying with small amounts of Sc and Nd elements on the microstructure and mechanical properties of Al-Mg-Mn alloy were systematically investigated. The results show that the grains of Al-Mg-Mn alloy can be refined by the addition of minor Sc and Nd. Adding 0.2wt.% Sc or 0.2wt.% Nd element to Al-Mg-Mn alloy can improve the strength and recrystallization temperature. Especially, after a combined addition of 0.1wt.% Sc and 0.1wt.% Nd, owing to the Al16Mg7Nd phase formed in the alloy, which pinned at the grain boundary can hinder the migration of the grain boundary during annealing process, the recrystallization temperature of the Al-Mg-Mn alloy is increased by 100°C, and the increments of tensile strength and yield strength are 65 and 55MPa, respectively. KeywordsAl-Mg-Mn alloy–mechanical properties–microstructure–Nd–Sc

Ranjit Bauri et al. (2015) observed that no defect obtained at tool rotational speed of 1200 rpm and traverse speed of 24 mm/min and vertical load 8kN for in 5083 Al+Ni particles metal matrix composite.

In the present study Ni particles were incorporated in 5083 Al alloy by friction stir processing (FSP) to fabricate metal particle reinforced composite. A conventional cylindrical tool was first used for FSP and several processing parameters (rotational and traverse speeds) were explored to get a defect free stir zone and uniform distribution of the particles. The effect of tool geometry was also studied by using another tool having special features on the pin and the shoulder.A tool rotation speed of 1200

rpm and traverse speed of 0.4 mm/s were found to be optimum for obtaining a defect free stir zone. However, the distribution of Ni particles was inhomogeneous for all the parameters used with the plain cylindrical tool irrespective of defective or a sound stir zone.The tool with the special features, threads on the pin and spiral grooves on the shoulder, was found to be very effective in both producing a sound stir zone and dispersing the Ni particles. It was also found that ball milled fine particles were dispersed more uniformly in the stir zone compared to the as-received coarse particles. FSP also refined the grain size of the aluminum matrix from 25μm to 3μm. The microstructure was characterized by equiaxed fine grains with a high fraction of high angle grain boundaries and a narrow grain size distribution. The effect of the particle incorporation on the mechanical properties of the alloy was also investigated. The strength increased significantly compared to the base alloy and more importantly a high amount of ductility was also achieved in the composite.

D. A. Zhemchuzhnikova (2016) The tensile strength and fatigue properties of alloy 1575 of the Al – Mg – Sc system are studied after hot deformation (at 360°C) and subsequent cold rolling with different reduction ratios. The effect of the deformed structure on the properties and mechanisms of fracture of the alloy under cyclic tests is determined and studied that cold rolling increases the fatigue and tensile strength of the alloy.

The tensile strength and fatigue properties of alloy 1575 of the Al – Mg – Sc system are studied after hot deformation (at 360°C) and subsequent cold rolling with different reduction ratios. The effect of the deformed structure on the properties and mechanisms of fracture of the alloy under cyclic tests is determined.

Srinivasa Rao et al. (2018) studied the effect of minor additions of scandium and zirconium to Al-Mg-Mn alloys. They observed that Scandium (0.2 – 0.6 wt. %) and zirconium (0.1wt. %) addition introduces an appreciable improvement in the mechanical properties to mechanical properties of Al-Mg-Mn alloys.

The effect of Sc and Zr on the superplastic properties of Al-Mg-Mn alloy sheets was investigated by a control experiment. The superplastic properties and the mechanism of superplastic deformation of the two alloys were studied by means of optical microscope, scanning electron microscope and transmission electron microscope. The elongation to failure of Al-Mg-Mn-Sc-Zr alloy is larger than

that of Al-Mg-Mn alloy at the same temperature and initial strain rate. The variation of strain rate sensitivity index is similar to that of elongation to failure. In addition, Al-Mg-Mn-Sc-Zr alloy exhibits higher strain rate superplastic properties. The activation energies of the two alloys that are calculated by constitutive equation and linear regression method approach the energy of grain boundary diffusion. The addition of Sc and Zr decreases activation energy and improves the superplastic property of Al-Mg-Mn alloy. The addition of Sc and Zr refines the grain structure greatly. The main mechanism of superplastic deformation of the two alloys is grain boundary sliding accommodated by grain boundary diffusion. The fine grain structure and high density of grain boundary, benefit grain boundary sliding, and dynamic recrystallization brings new fine grain and high angle grain boundary which benefit grain boundary sliding too. Grain boundary diffusion, dislocation motion and dynamic recrystallization harmonize the grain boundary sliding during deformation.

Srinivasa Rao et al. (2018) observed that the better mechanical properties are obtained at tool rotational speed of 1132 rpm and traverse speed of 26.26 mm/min and vertical load 9.6 kN for Al-Mg-Mn-Sc-Zr alloys .

Elena Avtokratovaa (2021) it is shown that after MIF followed by cold rolling, the outstanding combination of the tensile strength and ductility was observed concomitantly with the fatigue resistance superior to that in the contemporary alloys of the same class and/or of many currently available commercial high-strength alloys.

BinWang (2021) studied that the high-cycle fatigue (HCF) and fatigue crack propagation (FCP) characteristic in relation to the microstructure in the 5083-O aluminum alloy. The HCF strengths of the 5083-O Al alloy in parallel to rolling direction (PD) and vertical to rolling direction (VD) specimens are 164 MPa and 165 MPa, respectively, However, the FCP resistance of the specimens reveals evident anisotropy. The FCP resistance of the PD specimen is less than that of the VD specimen, which is predominantly caused by the main crack expanding along the chain-shaped coarse inclusions in the PD specimen. These chain-shaped coarse inclusions, particularly Fe/Mn containing particles with secondary microcracks, might accelerate FCP rate and decrease FCP resistance.

The objective of the present study is to investigate the high-cycle fatigue (HCF)and fatigue crack propagation (FCP)characteristic in relation to the microstructure in the 5083-O aluminum alloy. The

HCF strengths of the 5083-O Al alloy in parallel to rolling direction (PD)and vertical to rolling direction (VD)specimens are 164 MPa and 165 MPa, respectively, However, the FCP resistance of the specimens reveals evident anisotropy. The FCP resistance of the PD specimen is less than that of the VD specimen, which is predominantly caused by the main crack expanding along the chain-shaped coarse inclusions in the PD specimen. These chain-shaped coarse inclusions, particularly Fe/Mn containing particles with secondary microcracks, might accelerate FCP rate and decrease FCP resistance.

Nikolay BELOV (2017) studied Effect of 0.3% Sc on microstructure, phase composition and hardening of Al-Ca-Si eutectic alloys

The phase composition, microstructure and hardening of aluminum-based experimental alloys containing 0.3% Sc, 0–14% Si and 0–10% Ca (mass fraction) were studied. The experimental study (electron microscopy, thermal analysis and hardness measurements) was combined with Thermo-Calc software simulation for the optimization of the alloy composition. It was determined that the maximum hardening corresponded to the annealing at 300–350 °C, which was due to the precipitation of Al_3Sc nanoparticles with their further coarsening. The alloys falling into the phase region (Al)+Al_4Ca+Al_2Si_2Ca have demonstrated a significant hardening effect. The ternary eutectic (Al)+Al_4Ca+Al_2Si_2Ca had a much finer microstructure as compared to the Al–Si eutectic, which suggests a possibility of reaching higher mechanical properties as compared to commercial alloys of the A356 type. Unlike commercial alloys of the A356 type, the model alloy does not require quenching, as hardening particles are formed in the course of annealing of castings.

Liqiong Zhong (2018) studied High Cycle Fatigue Performance of Inconel 718 Alloys with Different Strengths at Room Temperature

In this paper, the high cycle fatigue performance of solid solution state and aged Inconel 718 superalloys was studied at room temperature. Scanning electron microscopy (SEM) and transmission electron microscopy (TEM) were used to analyze the original structural features and fatigue deformation features of two kinds of alloys. SEM, laser scanning confocal microscopy, and electron backscatter diffraction (EBSD) were used to analyze the secondary fracture features of the fatigue fracture morphology and fatigue fracture profile. The results showed that the aging treatment

significantly affected the strength and plasticity of the alloy, which in turn affected the fatigue performance of the alloy. After the aging treatment, the yield strength σ_s and the tensile strength σ_b of the Inconel 718 alloy increased by 152% and 65.9%, respectively, compared with those of the solid solution state, but the rate of elongation δ and rate of contraction in the cross-section area φ decreased by 63.7% and 52.3%, respectively. The fatigue limit of the aged state was lower than that of the solid solution state by 6.3%. An analysis of the fatigue fracture mechanism showed that the fatigue fractures before and after aging were all initiated in the grains oriented relatively unfavorably on the surface of the sample, with a mixture of intergranular and transgranular propagation after the transgranular propagation of several grains. The higher plasticity of the solid solution state Inconel 718 alloy resulted in a large number of slip deformation zones under high cycle fatigue loads, and the plastic deformation was relatively uniform. The lengths of the secondary fractures were as high as 120 μm, which formed the single-source plastic fatigue fracture that promoted an increase in the fatigue limit. After aging treatment, the higher strength of the Inconel 718 alloy made dislocation slip difficult under high cycle fatigue loads, and the plasticity compatible deformation capability was poor. When local dislocations slipped to the intragranular γ" phase, γ' phase, or interfaces with nonmetallic compounds (NMCs), plugging occurred. The degree of stress concentration increased, causing the initiation of fatigue fracture; the secondary fracture was approximately 20 μm. Brittle cleavage due to multiple sources significantly reduced the fatigue limit.

Esther T. Akinlabi (2020) studied Effects of processing parameters on mechanical, material flow and wear behavior of friction stir welded 6101-T6 and 7075-T651 aluminum alloys

Dissimilar friction stir welding (FSW) between 6101-T6 and 7075-T651 aluminum alloys was conducted. Three different parameters each were investigated for rotational speed and travel speed, and the effects of these parameters on the tensile behavior, hardness and wear were evaluated. The results indicate that the ultimate tensile strength increases with an increase in the feed rate. However, the increase in rotational speed decreases the ultimate tensile values. The fractured analysis of the tensile samples shows similarities in the fractured pattern as all the samples failed at heat-affected zone close to the 6101-T6 alloy. The hardness varies across the heat affected zones and nugget zone both at constant rotational speed and welding speeds. The highest resistance to wear occurred at

65 mm min^{-1} and 1850 rpm welding speed and rotational speed respectively while better material mixing was achieved at the nugget zone of the welds at 1250 rpm and 110 mm/min

2.2 SUMMARY

By studying several articles and publications available as mentioned above it is inferred as, Due to the addition of scandium and zirconium to Al-Mg-Mn alloy the refining of grain size become better, it resists to fatigue corrosion cracking, increases weldability and machinability, it increases the toughness of the material, desirable mechanical, tensile and fatigue properties.

It is inferred that, The Addition of Scandium may improve the grain refinement thus providing us with fine and well distributed grain size which will lead to several superior mechanical properties such as better fatigue life, weldability and machinability.

It is inferred that; the addition of Zirconium may improve the toughness of alloys and also decrease the fatigue corrosion cracking effect on materials subjected to cyclic loading.

3 OBJECTIVE AND METHODOLOGY

3.1 OBJECTIVE

The main objectives of the present work are to focus on fatigue failure of Al-Mg-Mn alloy with minor addition of scandium and zirconium where it is most needed.

3.2 METHODOLOGY

- Preparation of Al-Mg-Mn alloy and Al-Mg-Mn-Sc-Zr alloy plates using stir casting.
- Cold rolling the plates to obtain a flat specimen with desired thickness.
- Preparation of tensile and fatigue specimens under ASTM E8 standards for low cycle fatigue test.
- Al-Mg-Mn alloy and Al-Mg-Mn-Sc-Zr alloy specimens is tested for measurement of tensile and fatigue strength.

Fig 3.1 Fabrication process of Al-Mg-Mn alloy

(a) Electrical Resistance Furnace (b) Pouring molten mixture into the preheated permanent mould (c) Al-Mg-Mn-Sc-Zr as cast plate (d) Cold rolling of plate.

Fig 3.2 Water Jet Machining Live Picture of Specimen

4 EXPERIMENTATION

4.1 MATERIAL PREPARATION

In the present study, the aluminum alloys Al–4.2Mg– 0.6Mn alloy was produced by melting in an electrical resistance furnace. This alloy was prepared by stir casting, using Al–4.2Mg–0.6Mn alloy and three master alloys (Al-10wt% Mg, Al-2wt%Sc and Al–5wt% Zr), that was melted in alumina crucible and then poured into a metal mold. The final temperature of the melt was always maintained at 1000 ± 15°C with the help of the electronic controller. Then, the melt was homogenized under stirring at 900°C. Casting was done in mild steel metal mold with graphite paste (die coat) as mold releasing agent preheated to 200°C. After casting, the plates were machined into 150 X 150 X 6 mm^3 using water jet machining, then cold-rolled to 5 mm-thick sheets.

4.2 EXPERIMENTATION STEPS INVOLVED

The cold rolled Al-Mg-Mn-Sc-Zr plate was cut in standard specimen shapes and dimensions, the standard specimens for ultimate tensile strength, and fatigue test were machined from the fabricated plate. Specimen dimensions are as shown in Figure 4.1

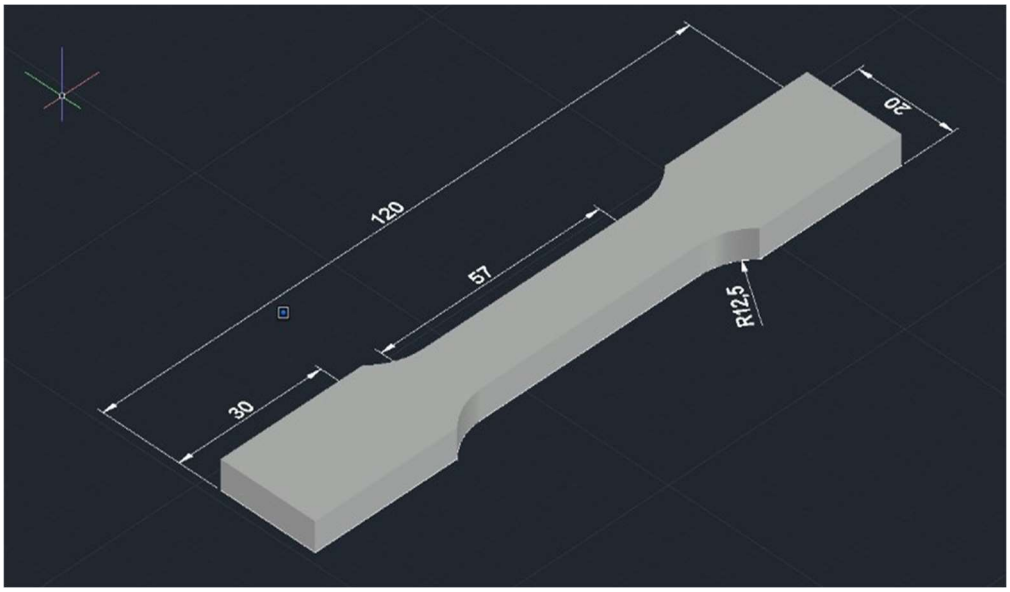

Fig 4.1 AutoCAD Rendering of Specimen

4.3 TENSILE TESTING

This was done so as to get the specimen tensile strength. This test was done in INSTRON 8801 is shown in figure 4.2. From this obtained data the fatigue test was done. Yield strength of the sample is obtained from this machine. Other related data are also obtained.

The tensile testing and fatigue failure is tested on THE INSTRON 8801 computerized universal testing machine for which after concluding the tensile test for specimens the yield strength is noted and the fatigue cycle load is applied at 40% of Yield Strength which is Standard testing method for aluminum 5 series 5083 alloys. The machine and its specifications are shown below.

4.3.1 SPECIFICATIONS OF THE MACHINE:

Tensile strength tester: Instron 8801

Applications: tensile, compression and bending tests

Type: mechanical tensile strength tester

Max. force: 100 kN tensile, 50 kN compression

Speed: 0.05 to 50 mm/min

Fig 4.1 INSTRON 8801 With SPECIFICATIONS

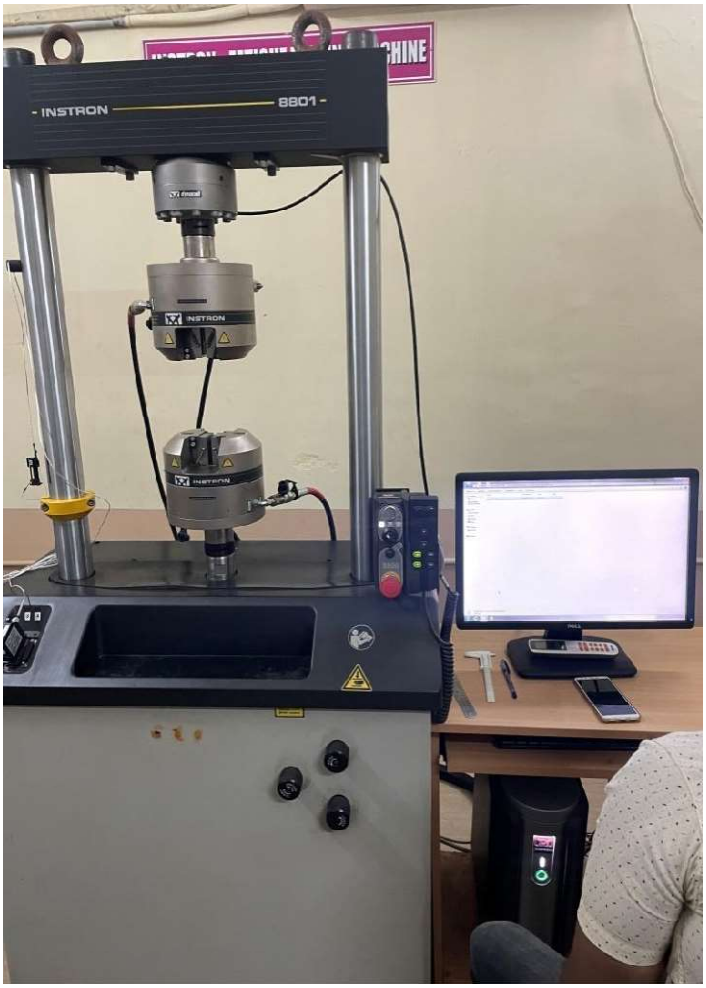

Fig 4.2 Universal testing machine

4.4 FATIGUE TESTING

After the calculation of yield stress is done, the specimen then would be treated in INSTRON 8801. In this fatigue life of the material is known. In this machine the number of cycles leading to failure of the material is known which gives the fatigue strength. This is a Electro-magnetic resonance machine capable of 50kN dynamic and 100kN static loading. Fitted with a DCPD system with PC based data acquisition. In this test the fatigue life of the specimen was determined for Al-Mg-Mn alloy and Al-Mg-Mn-Sc-Zr alloy.

In this machine the fatigue life of the specimen is calculated. The load applied here is 90% of the yield stress of the material.

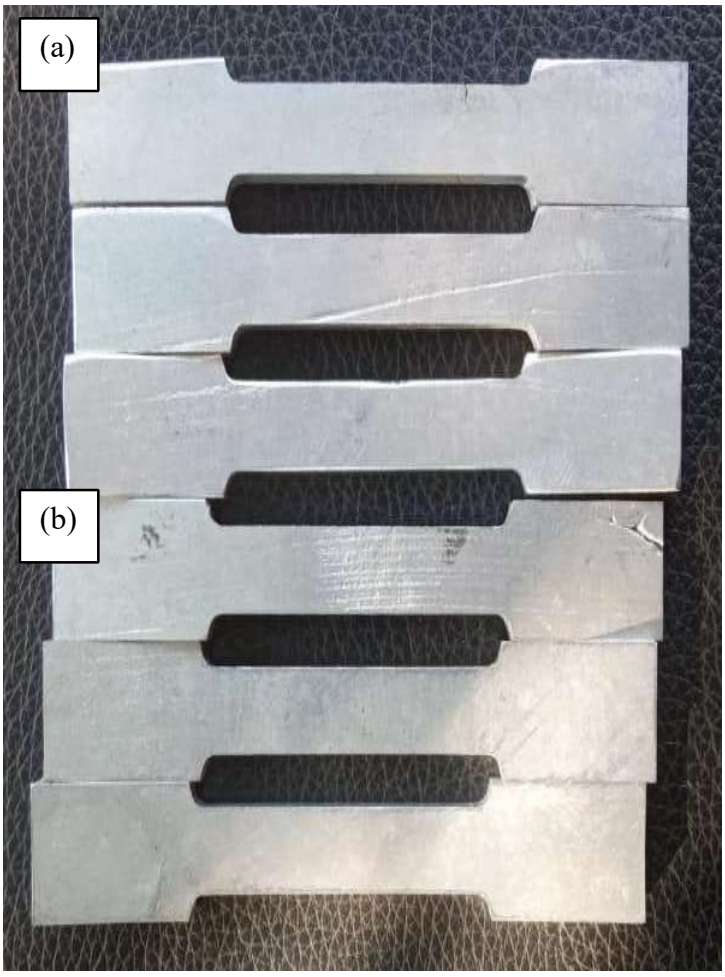

Fig 4.3 Before fatigue test: (a) Al-Mg-Mn alloy and (b) Al-Mg-Mn-Sc-Zr

Fig 4.4 After fatigue test Al-Mg-Mn alloy

Fig 4.5 After fatigue test Al-Mg-Mn-Sc-Zr alloy

5 RESULTS AND DISCUSSION

5.1 INTRODUCTION

The fabricated aluminum alloys were Al-Mg-Mn and Al-Mg-Mn-Sc-Zr alloys. The tensile testing of this specimen is done in INSTRON 8801.The tensile data obtained are tabulated in table 5.2. The results and discussions are presented in this Chapter

5.2 STUDY ON THE FABRICATED Al-Mg-Mn AND Al-Mg-Mn-Sc-Zr ALLOYS

5.2.1 BASE MATERIAL PROPERTIES

The chemical composition of the Al-Mg-Mn alloy is shown in Table 5.1and mechanical properties are tabulated in Table 5.2.

Table 5.1 Chemical composition of the fabricated alloys

Alloy type	**Mg**	**Mn**	**Si**	**Cr**	**Zn**	**Ni**	**Li**	**Sc**	**Zr**	**Bal.**
Al-Mg-Mn alloy	4.20	0.60	0.17	0.10	0.06	0.006	0.001	-	-	Al
Al-Mg-Mn-Sc-Zr alloy	4.18	0.53	0.14	0.04	0.05	0.005	0.001	0.41	0.11	Al

5.2.2 FINDINGS OF TENSILE TEST

Table 5.2 Mechanical Properties of the fabricated alloys

Alloy type	**UTS (MPa)**	**YS (MPa)**	**%E**
Al-Mg-Mn alloy	188.8	69.6	8.7
Al-Mg-Mn-Sc-Zr alloy	260.4	208.0	7.4

5.2.3 FINDINGS OF FATIGUE TEST

This is done at a stress value of about yield stress (YS). The specimens taken were applied to a load of about this high stress value.

Table 5.3 Life of the fabricated alloys

Maximum load	**Life (cycles)**	
	Al-Mg-Mn alloy	Al-Mg-Mn-Sc-Zr alloy
40% of YS	1247	32188

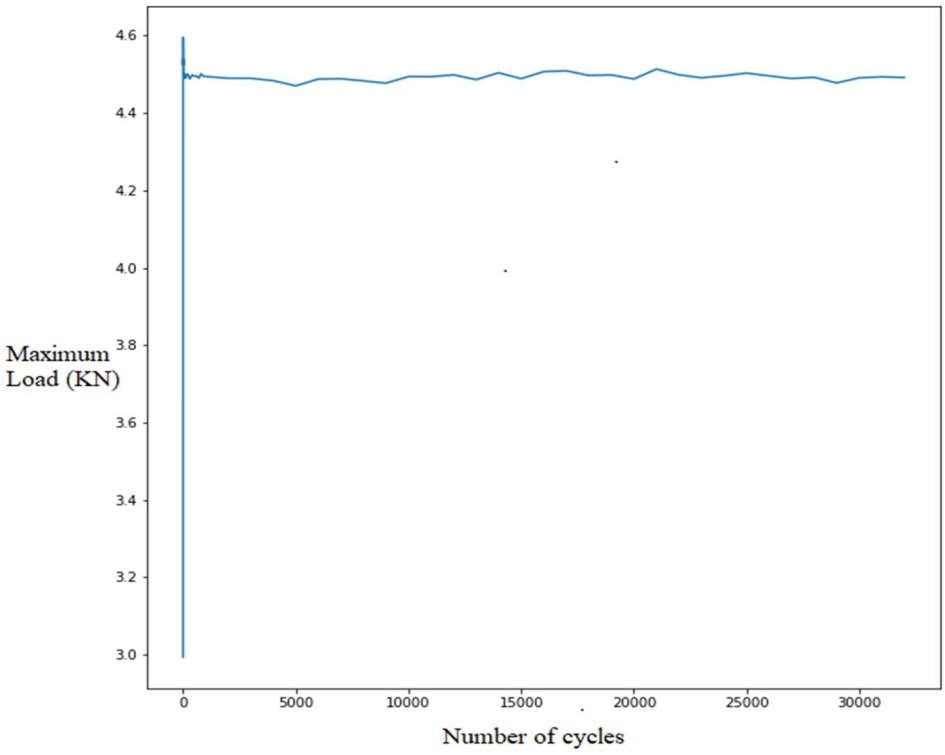

Fig 5.1 Maximum Load vs Number of Cycles

From the above graph it is evident that the tensile fatigue load is always fluctuating. So, it is organized to visualize the variation of maximum load applied in every cycle to the corresponding number of cycles.

The load applied rises from 3 KN to 4.6 KN in the first cycle and then it fluctuates in range of 4.4 KN to 4.6 KN throughout the testing phase. Initially a gradual tensile load of 3 KN is applied over the specimen. This initial load is applied carefully in order to prevent sudden impact.

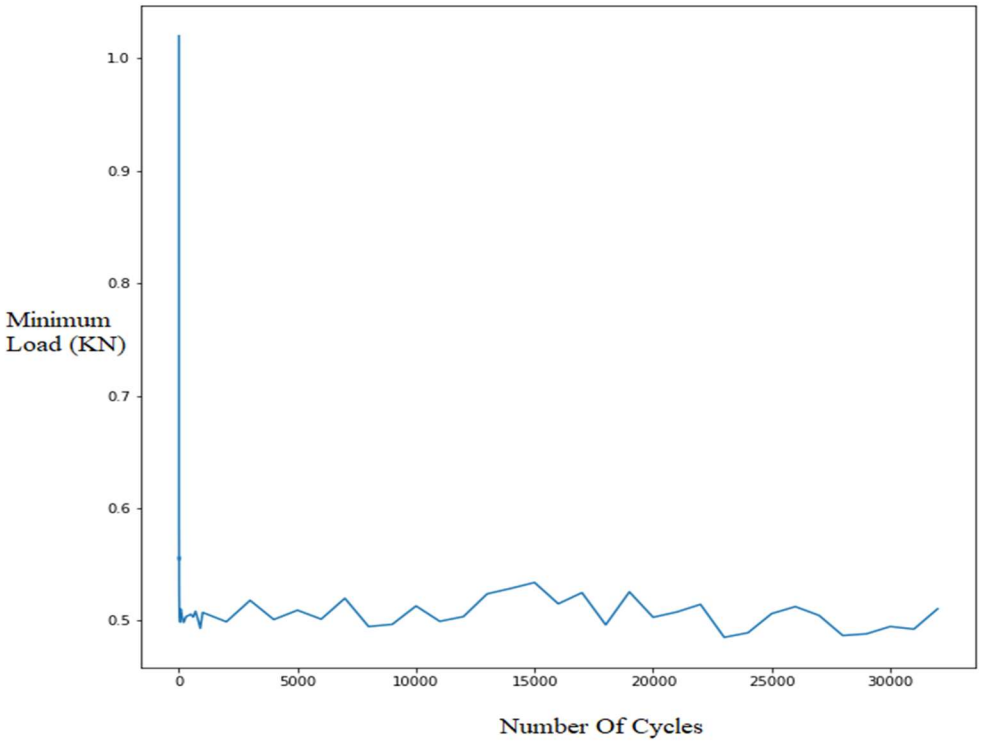

Fig 5.2 Minimum load vs Number of Cycles

In this Minimum Load vs Number of Cycles graph, it is observed that the load varies from 0.4 KN to 1.1 KN over the entire process from 0th cycle to 32188th cycle the load fluctuates over a small range with respect to number of cycles. The highest minimum load applied is found to be applied during the initial stage of testing. This is due to the initialization parameters set to the testing machine.

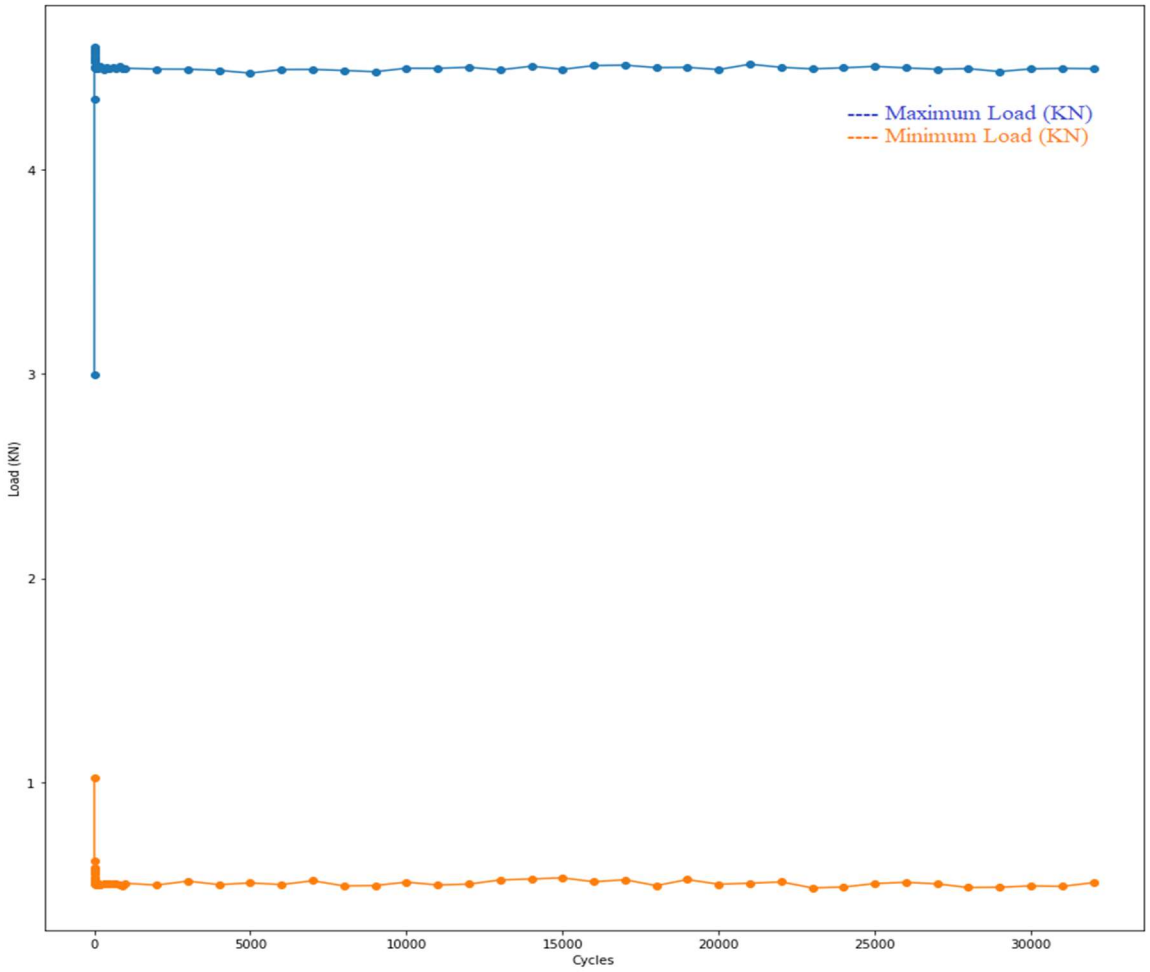

Fig 5.3 Maximum and Minimum load vs Number of Cycles

In the above graph it can be observed that there are two lines plotted with respect to the number of cycles in order to get a combined intuition that this graph is generated. The 'BLUE' line indicates the maximum load in the 'Load (KN)' axis and the 'ORANGE' line indicates the minimum load in the 'Load (KN)' axis both with respect to the number of cycles elapsed. A clear intuition is obtained regarding the variation of both 'Load' with elapsed cycles and its fluctuations.

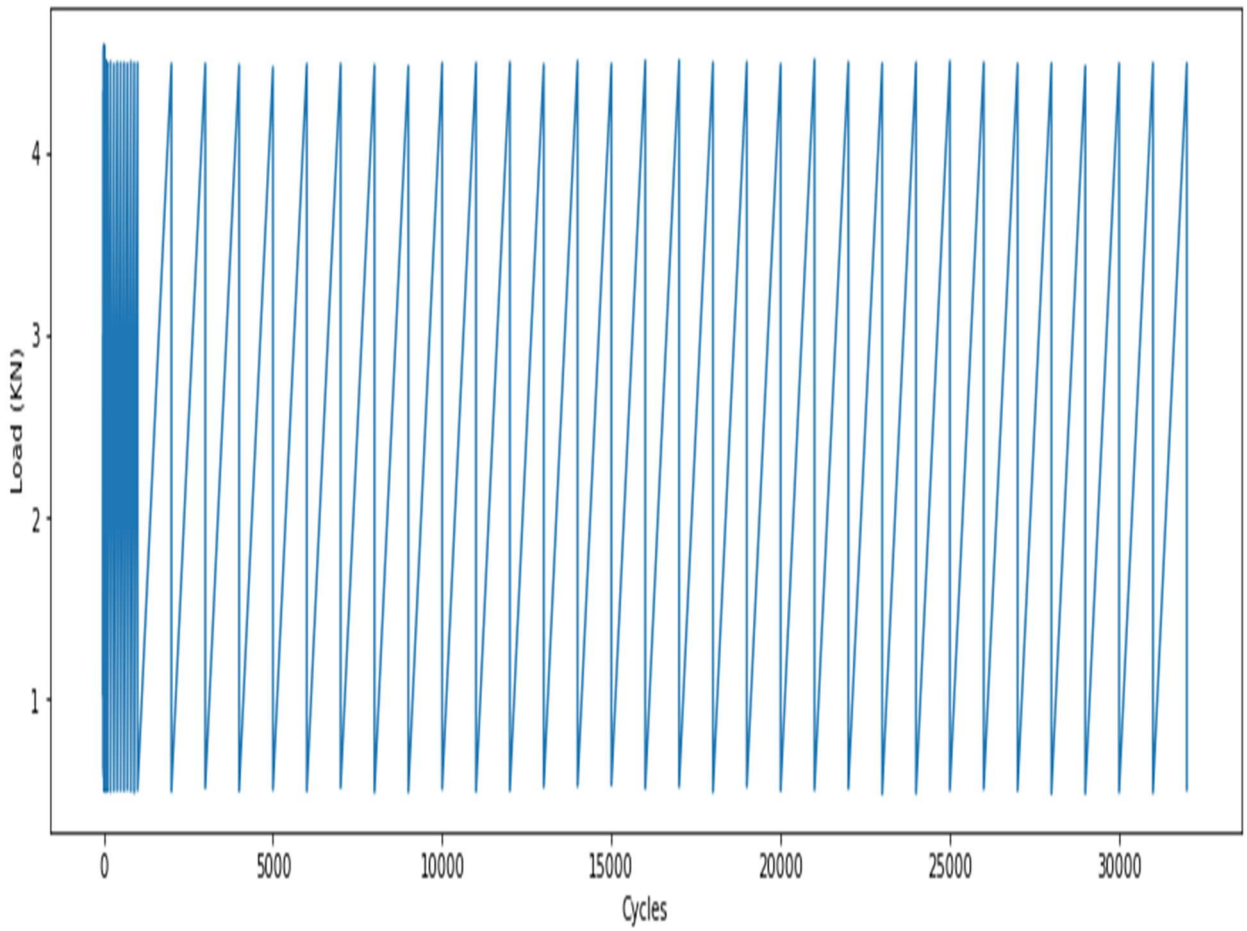

Fig 5.4 Load vs Number of Cycles

In the above graph the load and cycles are compared with each other. The load fluctuation of fatigue type loading is clearly visualized here in this graph.

The main objective of this graph is to explain the fatigue load characteristics with progression in elapsed time and number of cycles. The trend is clearly observed of increasing and decreasing load periodically; this is nothing but the fatigue load cycle plotted over the entire process.

5.3 COMPARISON OF TRENDS

Table 5.4 Comparison of Trends with Cyclic Load vs Elapsed Cycles

Elapsed_Cycles	Cyclic_Load_Al-Mg-Mn-Sc-Zr(kN)	Cyclic_Load_Al-Mg-Mn(kN)
1	2.993088309	4.637795966
1	1.01968497	2.235195134
2	4.344941396	6.172452681
2	0.617712922	1.742987428
3	4.595278855	6.535080448
3	0.580945611	1.680418104
4	4.582597967	6.598250847
4	0.576549117	1.670759171
5	4.575511999	6.573969685
5	0.569789764	1.613648143
6	4.561951105	6.542106904
6	0.553885568	1.63571341
7	4.548127018	6.534367334
7	0.557000376	1.584665757
8	4.530220851	6.531278323
8	0.53538233	1.568524912
9	4.523732048	6.527339481
9	0.530011393	1.58280246
10	4.539823998	6.523442734
10	0.524662994	1.534483302

20	4.500025045	6.464763265
20	0.505843945	1.51505461
30	4.4960659	6.476762611
30	0.503909308	1.492005773
40	4.493231792	6.479863822
40	0.509582646	1.527839806
50	4.491421115	6.469736993
50	0.501287542	1.502421591
60	4.500343185	6.495039817
60	0.4986763	1.501617394
70	4.499537311	6.501395535
70	0.510387868	1.50086144
80	4.491167236	6.51445929
80	0.509701855	1.521131396
90	4.498916026	6.488988362
90	0.503523182	1.485742256
100	4.489920381	6.489644386
100	0.506386813	1.472021081
200	4.500981886	6.504135858
200	0.498500094	1.506374311
300	4.488048796	6.498596631
300	0.503665674	1.484021917
400	4.498219397	6.490194611

400	0.504608639	1.490754727
500	4.494898953	6.495656073
500	0.505793747	1.505942736
600	4.495785479	6.487479806
600	0.503287371	1.505490672
700	4.490166809	6.504356209
700	0.50835982	1.49625754
800	4.501096159	6.484653894
800	0.501335319	1.495731622
900	4.494985472	6.495573837
900	0.493284687	1.506396197
1000	4.494236503	6.501343846
1000	0.507336855	1.491190307
2000	4.489660263	SPECIMEN FAILED!
2000	0.499095116	SPECIMEN FAILED!
3000	4.489572439	SPECIMEN FAILED!
3000	0.518098194	SPECIMEN FAILED!
4000	4.483469389	SPECIMEN FAILED!
4000	0.50106924	SPECIMEN FAILED!
5000	4.470082745	SPECIMEN FAILED!
5000	0.509336963	SPECIMEN FAILED!
6000	4.48760055	SPECIMEN FAILED!
6000	0.501416717	SPECIMEN FAILED!

7000	4.488470778	SPECIMEN FAILED!
7000	0.519948825	SPECIMEN FAILED!
8000	4.48294431	SPECIMEN FAILED!
8000	0.49483683	SPECIMEN FAILED!
9000	4.477027804	SPECIMEN FAILED!
9000	0.496805459	SPECIMEN FAILED!
10000	4.494049121	SPECIMEN FAILED!
10000	0.513144396	SPECIMEN FAILED!
11000	4.493635986	SPECIMEN FAILED!
11000	0.499488972	SPECIMEN FAILED!
12000	4.49855905	SPECIMEN FAILED!
12000	0.503673684	SPECIMEN FAILED!
13000	4.486155976	SPECIMEN FAILED!
13000	0.523895584	SPECIMEN FAILED!
14000	4.503754713	SPECIMEN FAILED!
14000	0.528732967	SPECIMEN FAILED!
15000	4.488667753	SPECIMEN FAILED!
15000	0.533976872	SPECIMEN FAILED!
16000	4.506742023	SPECIMEN FAILED!
16000	0.515066367	SPECIMEN FAILED!
17000	4.509050865	SPECIMEN FAILED!
17000	0.524932146	SPECIMEN FAILED!
18000	4.496972729	SPECIMEN FAILED!

18000	0.496348366	SPECIMEN FAILED!
19000	4.498317093	SPECIMEN FAILED!
19000	0.525645539	SPECIMEN FAILED!
20000	4.48771622	SPECIMEN FAILED!
20000	0.503082573	SPECIMEN FAILED!
21000	4.513446894	SPECIMEN FAILED!
21000	0.507783238	SPECIMEN FAILED!
22000	4.498535581	SPECIMEN FAILED!
22000	0.514518563	SPECIMEN FAILED!
23000	4.490908794	SPECIMEN FAILED!
23000	0.485262461	SPECIMEN FAILED!
24000	4.496110324	SPECIMEN FAILED!
24000	0.48930468	SPECIMEN FAILED!
25000	4.502945766	SPECIMEN FAILED!
25000	0.506335218	SPECIMEN FAILED!
26000	4.495753627	SPECIMEN FAILED!
26000	0.512536056	SPECIMEN FAILED!
27000	4.48910566	SPECIMEN FAILED!
27000	0.504716486	SPECIMEN FAILED!
28000	4.492024425	SPECIMEN FAILED!
28000	0.486867968	SPECIMEN FAILED!
29000	4.477605503	SPECIMEN FAILED!
29000	0.488359109	SPECIMEN FAILED!

30000	4.49089529	SPECIMEN FAILED!
30000	0.494860765	SPECIMEN FAILED!
31000	4.49328851	SPECIMEN FAILED!
31000	0.492552482	SPECIMEN FAILED!
32000	4.491741955	SPECIMEN FAILED!
32000	0.510581769	SPECIMEN FAILED!
32188	SPECIMEN FAILED!	SPECIMEN FAILED!

The primary intuition we obtain is the load fluctuations and how the fluctuations change with time. It is observed that the load curve has stopped near the 32188 cycles that indicates the failure of the specimen. It is the best depiction of the entire test with results of fatigue loading.

As seen in the table the difference between the number of cycles to failure of the specimens at an applied stress of 40% of the yield stress, is huge in terms of number of cycles. The failure of the investigated alloy here occurs at a very large number of cycles. This is of the order of 10^4. But the specimen with no addition of scandium and zirconium could not withstand and eventually a brittle fatigue failure occurred at 1247 cycles.

It can be found that, due to the addition of scandium to the aluminum the grain refinement turns fine that eventually delivers better fatigue behavior. Also due to the addition of zirconium to the aluminum, the toughness of investigated material has been increased substantially along with the fatigue corrosion cracking resistance. Due to these excellent mechanical properties imparted by these materials the fatigue resistance of investigated alloy has been superior to the alloy in which scandium and zirconium are not added. It can clearly be observed that the difference in the fatigue life of two materials is of the order 10^2. Hence it can be inferred that the addition of scandium and zirconium to the Al-Mg-Mn alloy improved the fatigue characteristics and imparted superior mechanical properties to the alloy.

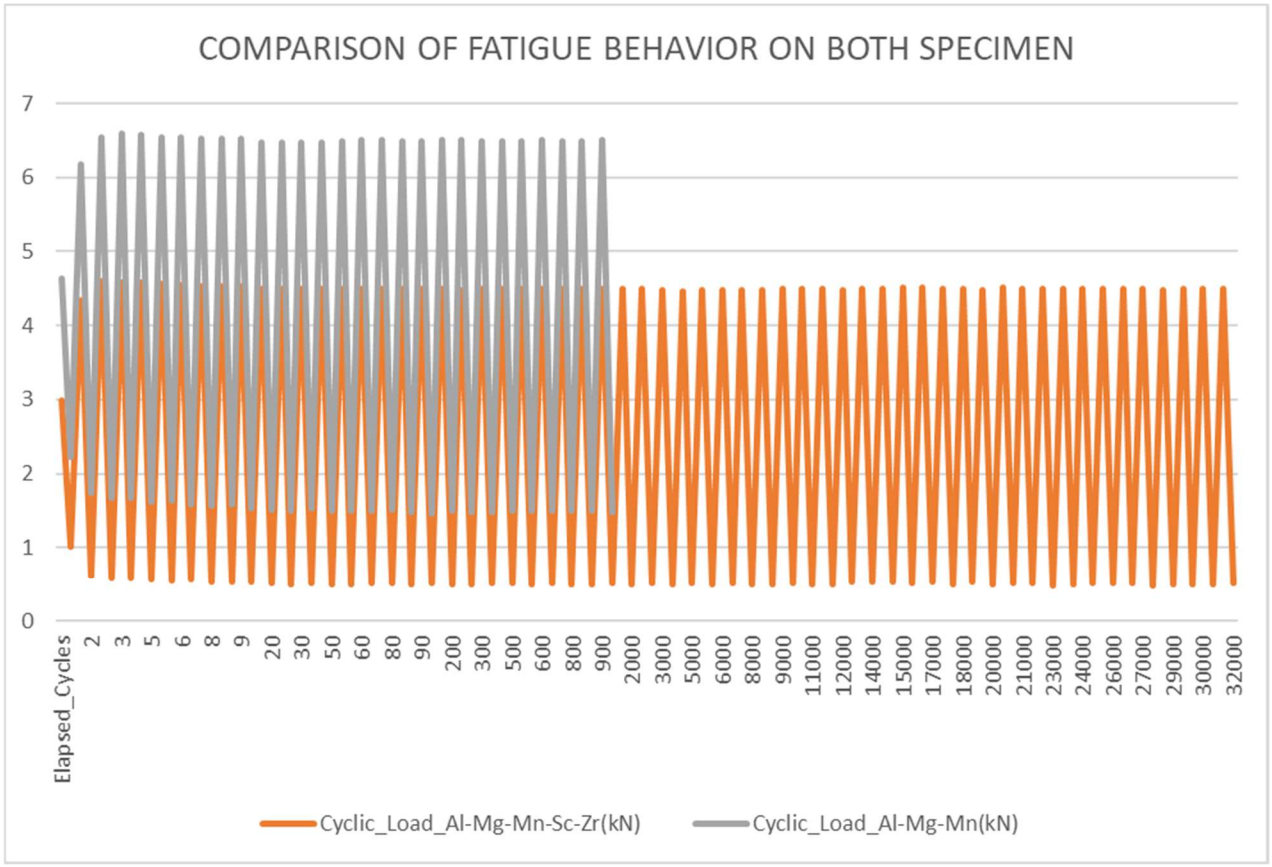

Fig 5.5 Comparison Chart for Fatigue

5.4 COMPARISON OF MAXIMUM AND MINIMUM LOADS

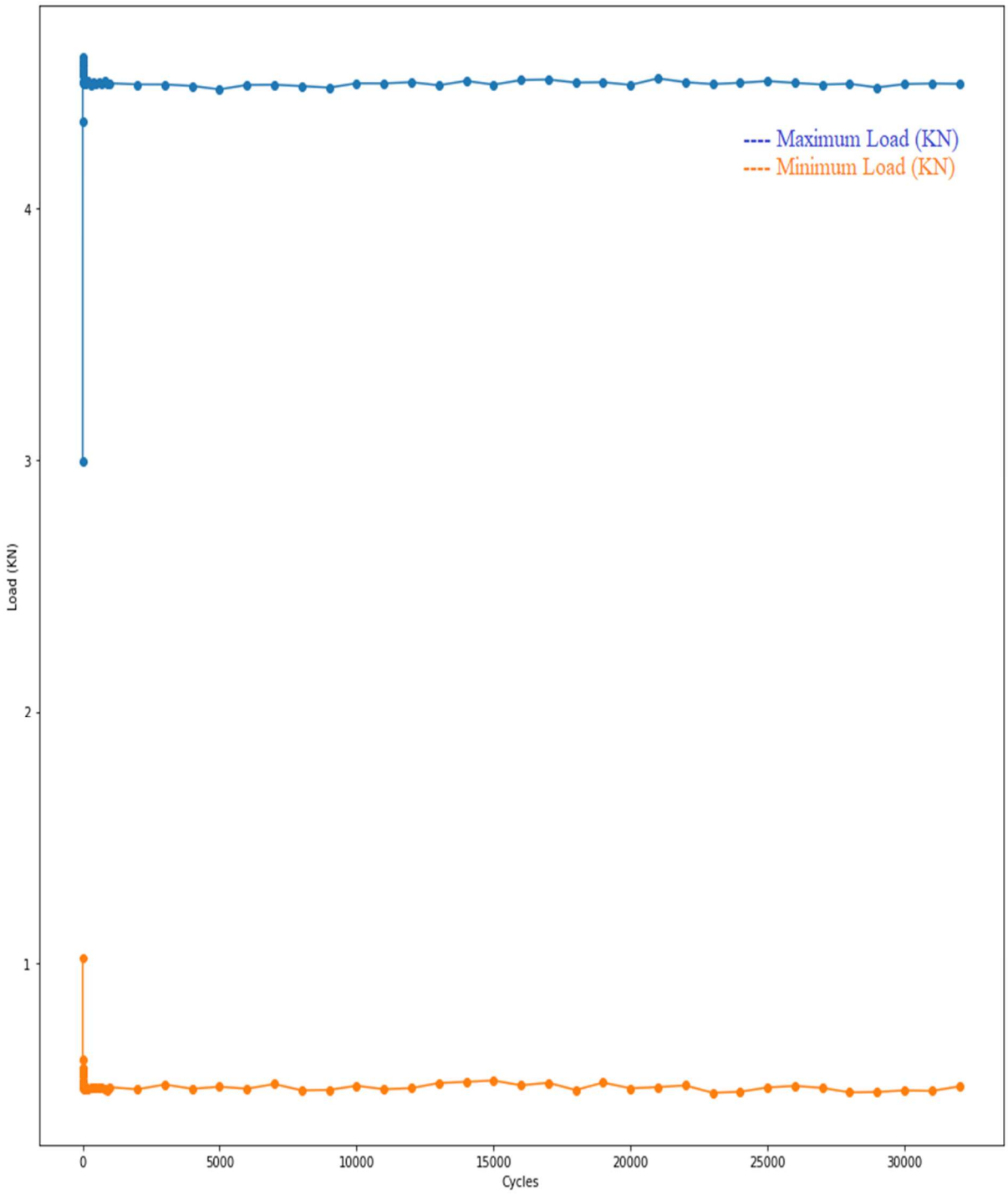

Fig 5.6 Cycles vs Max Load Al-Mg-Mn-Sc-Zr Specimen

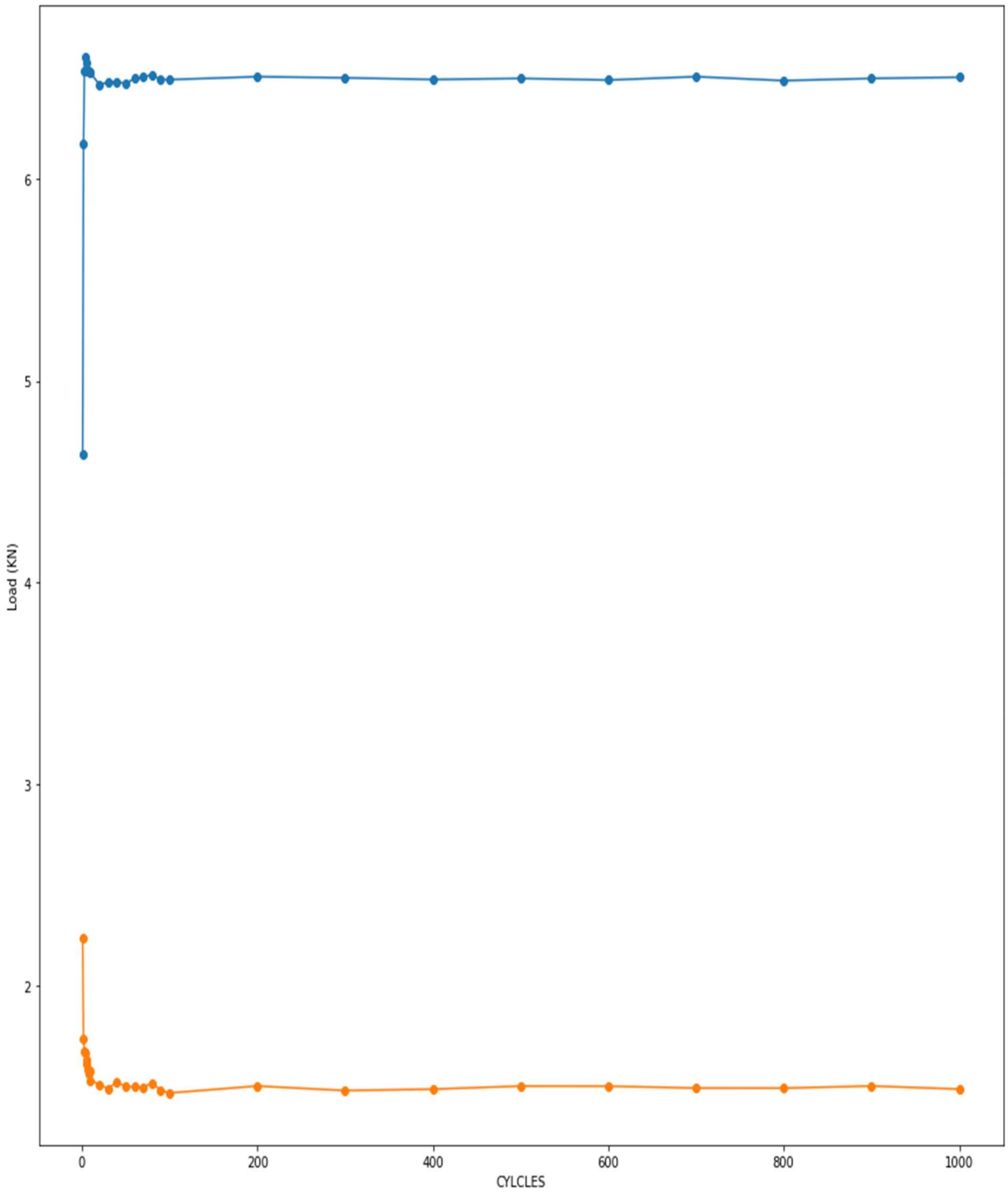

Fig 5.7 Cycles vs Max Load Al-Mg-Mn Specimen

The above figures, Figure 5.6 Cycles vs Max Load Al-Mg-Mn-Sc-Zr Specimen and Figure 5.7 Cycles vs Max Load Al-Mg-Mn Specimen. In the above graph it can be observed that there are two lines plotted with respect to the number of cycles in order to get a combined intuition that this graph is generated. The 'BLUE' line indicates the maximum load in the 'Load (KN)' axis and the 'ORANGE' line indicates the minimum load in the 'Load (KN)' axis both with respect to the number of cycles elapsed. A clear intuition is obtained regarding the variation of both 'Load' with elapsed cycles and its fluctuations. The above two graphs are computed using raw data of results of experiment conducted on both specimens. It is clearly evident the difference in the number of cycles the both specimens endured. The main objective is to get intuition on the variation of maximum load and minimum load with respect to elapsed cycles. Here it is observed the Alloyed specimen endured to much longer duration under prolonged fatigue loading which indicates the superior mechanical properties than the base alloy.

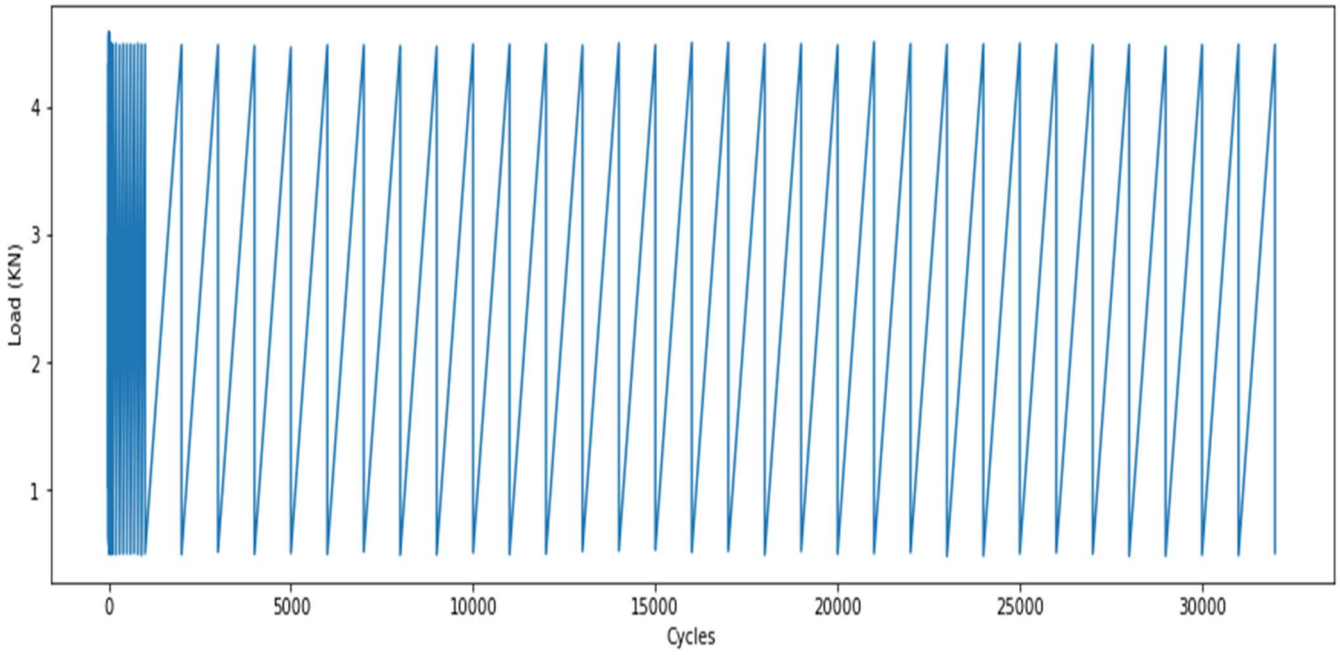

Fig 5.8 Elapsed Cycles vs Cycles Load Al-Mg-Mn-Sc-Zr Specimen

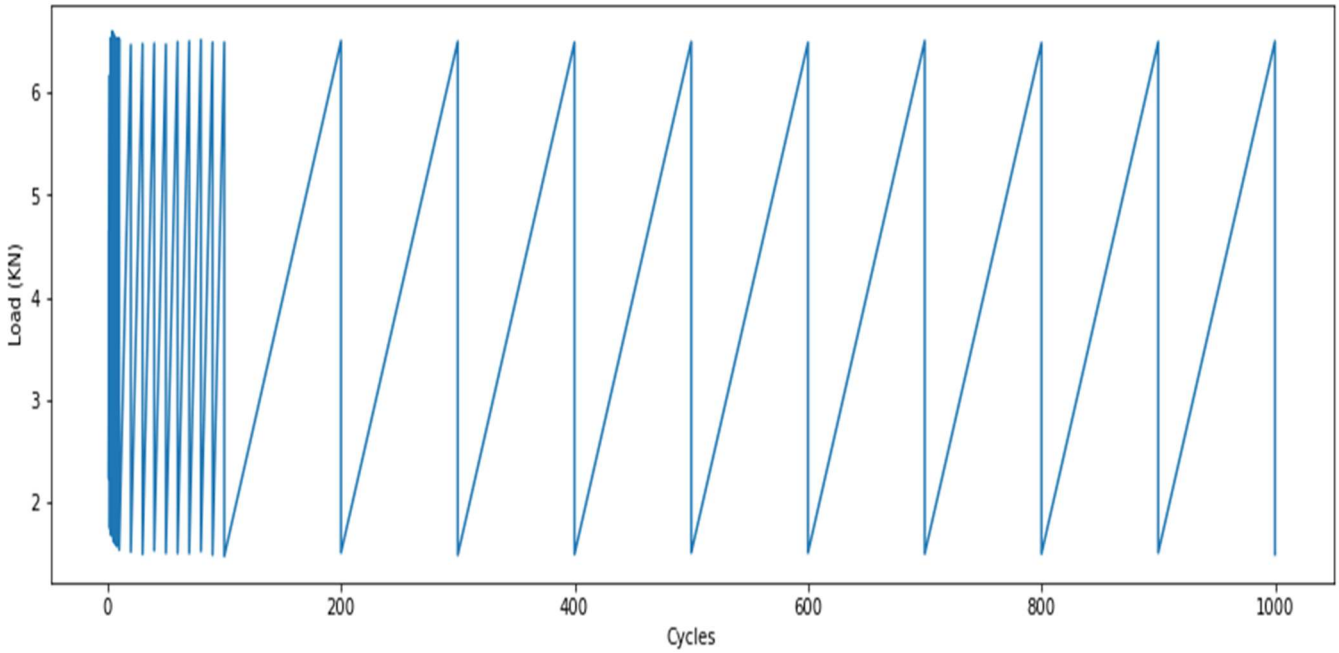

Fig 5.9 Elapsed Cycles vs Max Load Al-Mg-Mn Specimen

5.5 COMPARISON OF FATIGUE CYCLES

The figures, Figure 6.3 Elapsed Cycles vs Cycles Load Al-Mg-Mn-Sc-Zr Specimen and Figure 6.4 Elapsed Cycles vs Max Load Al-Mg-Mn Specimen. The load fluctuation of fatigue type loading is clearly visualized and compared here in these graphs. The main objective of this graph is to explain the fatigue load characteristics with progression in elapsed time and number of cycles. The trend is clearly observed of increasing and decreasing load periodically; this is nothing but the fatigue load cycle plotted over the entire process.

The specimen with no added Scandium and Zirconium performed very poorly compared to the specimen that contains Scandium and Zirconium. This graph comparison indicates the point where the specimen failed under repeated cyclic loading. It is seen that addition of aforementioned elements improved the fatigue life by orders of magnitude 100 times nearly.

As seen in the resulting graphs, the difference between the number of cycles to failure of the specimen at an applied stress of 40% yield strength is very large in the number of cycles. The failure of the alloy studied here occurs at a very large number of cycles. This is the order of 10^4. But the test piece has no scandium added and the zirconium is unable to resist and finally a brittle fatigue

fracture occurs at cycle 1247. For the investigated alloy Al-Mg-Mn-Sc-Zr Specimen the fatigue fracture occurs at 32188 cycles. Clearly it is observed drastic improvement in the fatigue life due to the addition of scandium and zirconium.

It can be seen that here, due to the addition of scandium in aluminum, the refining of the grain becomes better, which leads to better fatigue behavior. Also due to the addition of zirconium to aluminum, the toughness of the studied material has increased significantly as well as the resistance to fatigue. Due to the excellent mechanical properties imparted by these materials, the fatigue strength of the alloy studied is superior to that of the alloy. where scandium and zirconium are not added. It can be clearly observed that the difference in fatigue life of the two materials is order 10^2. Therefore, it can be inferred that the addition of scandium and zirconium to the Al-Mg-Mn alloy improved the fatigue and transmission properties of the alloys. superior mechanical properties for the alloy.

6 CONCLUSION AND FUTURE SCOPE

6.1 CONCLUSION

- The addition of Scandium and Zirconium eventually increased the Fatigue life of the investigated alloy compared to base alloy.
- The alloy with added Scandium and Zirconium is able to withstand the applied cyclic loads for 10^2order of cycles more than the base alloy.
- This indicates the grain refinement property of Scandium worked on the alloy and made the alloy more reliable and withstand fatigue load for a longer period of time.
- The added Zirconium's fatigue cracking rate reduction property made an impact on the investigated alloy's Fatigue life by slowing down the possible corrosion cracking due to fatigue loading condition.

6.2 FUTURE SCOPE

- The **TENSILE** properties can be determined for the fabricated alloys at different temperatures.
- The **FATIGUE** properties can be determined for the fabricated alloys at different temperatures.

7 REFERENCES

1. **Belov I. A. and Alabin, A. I.** "Advanced Aluminum Alloys with Zirconium and Scandium," Tsvetan. Met., No. 2, 99–106 (2007).
2. **BinWang (2021)** studied that the high-cycle fatigue (HCF) and fatigue crack propagation (FCP) characteristic in relation to the microstructure in the 5083-O aluminum alloy.
3. **C Watanabe** Al-Mg-Sc alloy polycrystals bearing Al3Sc particles with different sizes, i.e. 4, 6 and 11 nm in diameter, have been cyclically deformed at 423 K under constant plastic-strain amplitudes, and the microstructural evolution has been investigated in relation to the stress-strain response. (2009)
4. **D. A. Zhemchuzhnikova** The tensile strength and fatigue properties of alloy 1575 of the Al – Mg – Sc system are studied after hot deformation (at 360°C) and subsequent cold rolling with different reduction ratios. The effect of the deformed structure on the properties and mechanisms of fracture of the alloy under cyclic tests is determined and studied that cold rolling increases the fatigue and tensile strength of the alloy. (2016)
5. **Elena Avtokratovaa**The processing route towards outstanding performance of the severely deformed Al–Mg–Mn-Sc-Zr alloy.Materials Science and Engineering: AVolume 806, 4 March 2021, 140818
6. **Huizhong Li** Effect of Sc and Nd on the Microstructure and Mechanical Properties of Al-Mg-Mn Alloy Journal of Materials Engineering and Performance volume 21, pages 83–88 (2012)
7. **Yang Dongxia, Lixiaoya, Hedingyong, Huanghui**, "Effect of minor Er and Zr on microstructure and mechanical properties of Al–Mg–Mn alloy (AA5083) welded joints", Materials Science & Engineering A 561 (2013) 226–231.
8. **Mandal N.R**. (2005), 'Aluminum Welding', 2nd edition, Narosa Publishing Home Pvt. Ltd, Delhi.
9. **Norman et al.** investigated that small addition of scandium (Sc) in Al-aerospace alloys (AA2024 and AA7475). They studied the mechanical properties of these alloys. (2003)
10. **Norman A.F, Hyde K., Costello F., Thompson S., Birley S. ,Prangnell P.B.,** "Examination of the effect of Sc on 2000 and 7000 series aluminum alloy castings: for improvements in

fusion welding" Materials Science and Engineering: A, Volume 354, Issues 1–2, 15 August 2003, Pages 188-198

11. **He Zhen-bo, PENG Yong-yi, YIN Zhi-min, LEI Xue-feng**," Comparison of FSW and TIG welded joints in Al-Mg-Mn-Sc-Zr alloy plates" Trans. Nonferrous Met. Soc. China 21 (2011)1685-1691.
12. **Polmear I.J.**, Light Alloys: From Traditional Alloys to Nanocrystals, 4th ed., Butterworth-Heinemann/Elsevier, UK, 2006.
13. **Ranjit Bauri et al**. observed that no defect obtained at tool rotational speed of 1200 rpm and traverse speed of 24 mm/min and vertical load 8kN for in 5083 Al+Ni particles metal matrix composite. (2015)
14. **S.E.Stanzl-Tschegg** Fatigue and fatigue crack growth of aluminum alloys at very high numbers of cycles. volume 23, supplement 1, 2001, pages 231-237
15. **Shahrum Abdullah** Fatigue Crack Growth Simulation of Aluminum Alloy under Cyclic Sequence Effects 2011b DOI:10.5772/14898 2011
16. **Srinivasa Rao. K, Naga Raju P., Reddy G.M., and Prasad Rao K.** (2010). Microstructure and impression creep of age hardenable AA2219 aluminum alloy modified by Sc, Mg and Zr additions, Trans. Indian Inst. Metals, Vol. 63, No. 2-3, pp.379-384.
17. **Srinivasa Rao et al**. (2018) observed that the better mechanical properties are obtained at tool rotational speed of 1132 rpm and traverse speed of 26.26 mm/min and vertical load 9.6 kN for Al-Mg-Mn-Sc-Zr alloys . (2018)
18. **M. Srinivasa Rao and N. Ramanaiah**, "Effect of Scandium and Zirconium Additions on Mechanical Properties of Al-Mg-Mn Alloy", Transactions of The Indian Institute of Metals, Springer India Publications, ISSN-0975-1645, January 2019 Volume 72, issue 1, pp.227-238. doi: 10.1007/s12666-018-1476-8.
19. **Ranjit Bauri, G. D. Janaki Ram, Devinder Yadav, C. N. ShyamKumar(2015)**. Effect of process parameters and tool geometry on fabrication of Ni particles reinforced 5083 Al composite by friction stir processing, Materials Today: Proceedings 2 (2015) 3203 – 3211
20. **Zhang Zhijun** Influence of Erbium on Fatigue Behavior of Al-4.7Mg-0.7Mn-0.4Er-0.1Zr Alloy College of Material Science and Engineering,Beijing University of Technology,Beijing 100124,China.

21. **Nikolay BELOV (2017)** studied Effect of 0.3% Sc on microstructure, phase composition and hardening of Al-Ca-Si eutectic alloys

22. **Liqiong Zhong (2018)** studied High Cycle Fatigue Performance of Inconel 718 Alloys with Different Strengths at Room Temperature

23. **Esther T. Akinlabi (2020)** studied Effects of processing parameters on mechanical, material flow and wear behavior of friction stir welded 6101-T6 and 7075-T651 aluminum alloys